Clays and Clay Minerals, Vol. 37, No. 6, 497–510, 1989.

ZEOLITES IN PRE-CALDERA PYROCLASTIC ROCKS OF THE SANTORINI VOLCANO, AEGEAN SEA, GREECE

PANAYOTA TSOLIS-KATAGAS AND CHRISTOS KATAGAS
Department of Geology, University of Patras, 261 10 Patras, Greece

Abstract—The vitric matrix of pre-caldera acid tuff and tuff breccia of the Santorini volcano, Aegean Sea, Greece has been generally replaced by one or more of the following authigenic minerals: K-rich and (K,Ca)-rich clinoptilolite, mordenite, opal-CT, and clay minerals. Halite is also present in some samples. Initial compositional inhomogeneities between the dacitic blocks in tuff breccia and tuff seem to have controlled the type of K-rich heulandite-group zeolite that formed. Mordenite postdates the heulandite-group zeolites and opal-CT. Some mordenite has replaced the rims of glass shards. The alteration minerals are not related to vertical or lateral zonation, and the irregular distribution of their assemblages is attributed to variations in heat flow, ionic activity in interstitial waters, and permeability. The pyroclastic rocks were in a region of active heat flow during and after their emplacement. The formation of authigenic silicates may have led to the sealing of open spaces and fractures, imposing barriers to permeability and subdividing the original open system into smaller closed systems. As alteration progressed, some of the trapped water in each individual domain was consumed in hydration reactions. Salts could have been concentrated by such a process, and halite probably precipitated from solutions of appropriate composition in the individual closed systems.

Key Words—Clinoptilolite, Diagenesis, Mordenite, Pyroclastic, Tuff, Zeolite.

Περίληψη — Η υελώδης μάζα των προ-καλδερικών οξίνων τόφφων και τοφφικών λατυποπαγών του ηφαιστείου της Σαντορίνης, Αιγαίον Πέλαγος, Ελλάς, έχει γενικά αντικατασταθεί από ένα ή περισσότερα από τα ακόλουθα αυθιγενή ορυκτά: πλούσιο σε K- και (K, Ca)-κλινοπτιλόλιθο, μορντενίτη, οπάλιο-CT, και αργιλικά ορυκτά. Αλίτης εμφανίζεται επίσης σέ μερικά δείγματα. Ο τύπος του κλινοπτιλόλιθου που σχηματίζεται ελέγχεται από τις διαφορές των χημικών συστάσεων μεταξύ των δακιτικών θραυσμάτων των τοφφικών λατυποπαγών και των τόφφων. Ο μορντενίτης σχηματίζεται μετά το σχηματισμό των ζεολίθων της ομάδας του χεουλανδίτη και του οπάλιου-CT· μερικοί κρύσταλλοι μορντενίτη φαίνεται να αντικαθιστούν τα άκρα των θραυσμάτων υέλου. Η κατανομή των ορυκτών της εξαλλοίωσης δεν παρουσιάζει κατακόρυφη ή οριζόντια ζώνωση και η τυχαία εμφάνιση των διαφόρων ορυκτολογικών παραγενέσεων αποδίδεται σε μεταβολές της θερμικής ροής, της ενεργότητας των ιόντων στο νερό των πόρων και της διαπερατότητας. Τα πυροκλαστικά πετρώματα βρέθηκαν σε μια περιοχή ενεργής θερμικής ροής κατά τη διάρκεια και μετά την απόθεσή τους. Ο σχηματισμός των αυθιγενών πυριτικών ορυκτών είναι δυνατόν να προκάλεσε το κλείσιμο διακένων και ρωγμών στη μάζα των πυροκλαστικών, την ελάττωση της διαπερατότητας και τη διαίρεση του αρχικού ανοικτού συστήματος σε μικρότερα κλειστά συστήματα. Η συνέχιση της εξαλλοίωσης είχε σαν αποτέλεσμα μέρος του εγκλωβισμένου στις μικροπεριοχές νερού να καταναλώνεται σε ενυδατωτικές αντιδράσεις. Με τη διεργασία αυτή είναι δυνατή η συγκέντρωση αλάτων σε κάποια από τα κλειστά συστήματα και ο αλίτης είναι πιθανόν να δημιουργήθηκε σ'αυτά από διαλύματα κατάλληλης σύστασης.

INTRODUCTION

Clinoptilolite and mordenite are common authigenic minerals in sedimentary rocks of volcanic origin. Deposits of these zeolites have been reported throughout the world (Hay, 1966; Sheppard, 1971; Iijima and Utada, 1971; Gottardi and Obradović, 1978), but it was not until 1981 that the first zeolite deposit was discovered in Greece (Kanaris, 1981). The deposit occurs in the pre-caldera acid pyroclastic rocks (Lumaravi-Archangelos volcanics) of the Santorini Volcano, exposed along the southwestern edge of the Thera Island (Figure 1). According to Kanaris (1981), clinoptilolite, mordenite and analcime (?) formed in these pyroclastic rocks from constituents dissolved from volcanic glass.

Apart from a Kanaris' (1981) report on the occurrence of this deposit and a brief description of its mineralogical and geochemical characteristics based on five samples, no further data are available. The numerous eruptive events of the Santorini volcano from the Pleistocene to present (Nicholls, 1971; Ferrara *et al.*, 1980) suggest that the Lumaravi-Archangelos pyroclastic rocks were in a region of active heat production during and after their emplacement. Zeolites in geothermal areas commonly show a vertical zonation in mineral assemblages; but such a zonation has not been ob-

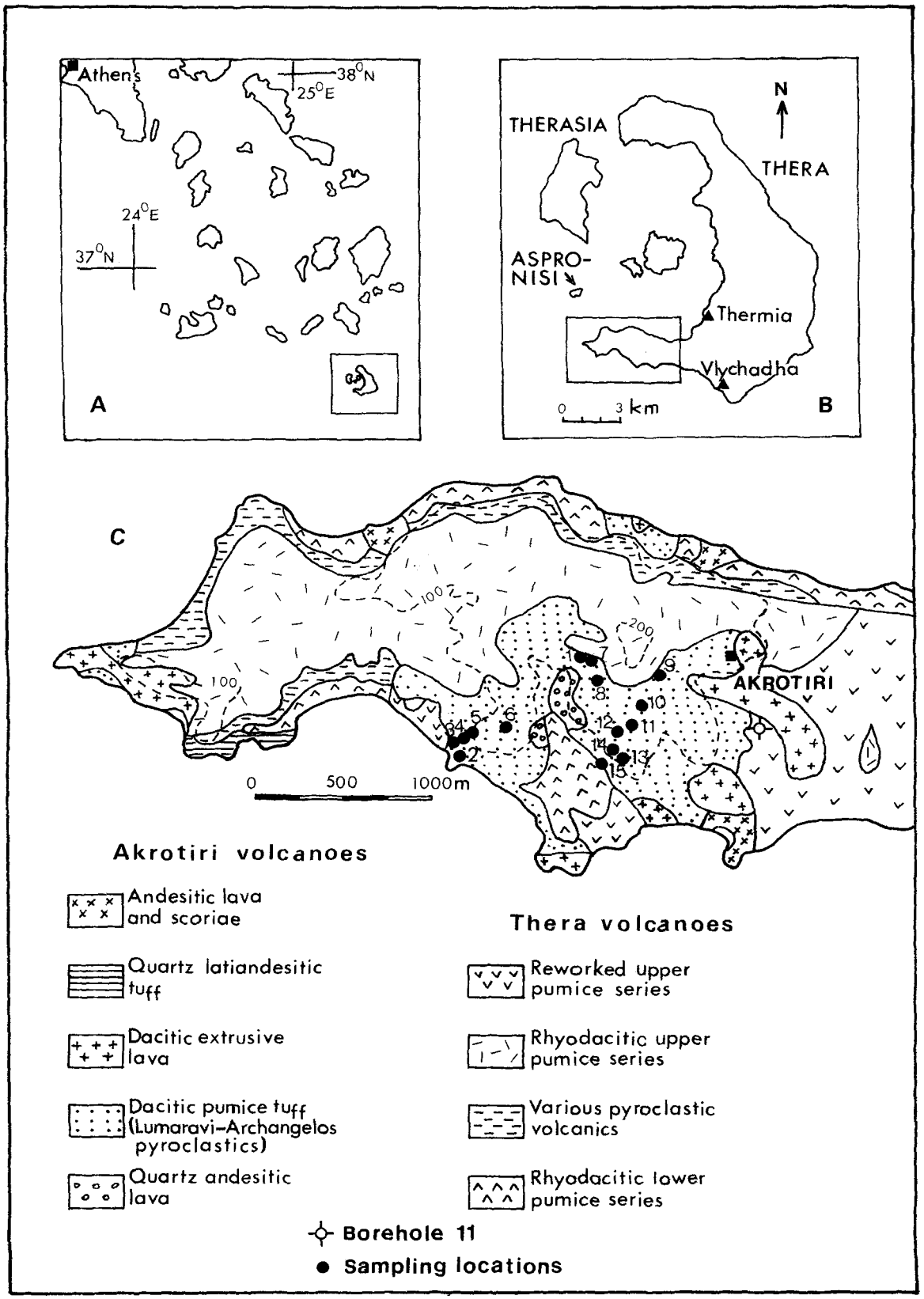

https://doi.org/10.1346/CCMN.1989.0370601 Published online by Cambridge University Press

served in the Lumaravi-Archangelos zeolite deposit. Recent work on the chemistry of the geothermal fluids in the area (Kavourides *et al.*, 1982) could provide a better understanding of the role of the interstitial, low-temperature saline solutions in the formation of the various zeolite-bearing assemblages. We here document new representative chemical and mineralogical data based on the study of about 60 samples collected from the Lumaravi-Archangelos zeolitic pyroclastic rocks. The investigation of these samples was made primarily to study the composition of the zeolites and the factors controlling the formation and the irregular distribution of the authigenic mineral assemblages.

GEOLOGIC SETTING

The volcanic formation of the Santorini group of islands are part of the Aegean volcanic arc, which became active during the Pliocene and reached its maximum activity during the Quaternary (Fytikas *et al.*, 1976; Barberi *et al.*, 1977; Innocenti *et al.*, 1979; Ferrara *et al.*, 1980). Santorini itself is an active volcano and has erupted numerous times prior to 1950. Prior to late Minoan time, the island was called Strongyle. About 1500 B.C., violent eruptions led to the collapse of the former circular island and to the formation of a large submarine caldera (11 × 7 km) enclosed by three remnants of the former stratocone, the islands Thera, Therasia, and Aspronisi. Two smaller islands then formed within the Santorini caldera by submarine and subaerial activity from about 197 B.C. to the present (Figure 1B). The calk-alkaline, high-alumina, basalt-andesite-dacite type of volcanism was mainly concentrated around eight centers (Reck, 1936; Pichler and Kussmaul, 1972), but was first restricted to the Akrotiri peninsula on the southwestern part of Thera (Figure 1C). The eruptive rocks of this peninsula consist of the silicic Lumaravi-Archangelos volcanics and the mafic Akrotiri volcanics. The former consists of minor flows of hornblende dacite and chiefly silicic pyroclastic rocks, which are zeolitic. The Akrotiri volcanics consist mainly of small domes and flows of basalts and andesites (Nicholls, 1971; Pichler and Kussmaul, 1972). Radiometric dating obtained on a dacitic lava flow from the oldest pre-caldera volcanic sequence is consistent with Pleistocene ages of 1.59 to 0.6 Ma. The volcanic products overlie a basement of Upper Triassic marble (Papastamatiou, 1958), which is overthrust on metapelites and metapsammites of Eocene age (Tataris, 1964) that are metamorphosed to greenschist-blueschist facies (Davis and Bastas, 1980; C. Katagas, Department of Geology, University of Patras, Patras, Greece, unpublished data, 1986). Recent work reveals that the island is geothermally active, with a geothermal gradient in its southern part of 1.6°C/10 m (Kavourides *et al.*, 1982).

The pyroclastic rocks cover an area of about 1 km² west of Akrotiri village (Figure 1C). The exposed thickness of the formation is about 160 m, but borehole data suggest a thickness of at least 220 m. The pyroclastic rocks do not seem to have originally accumulated in a marine or lake environment because the deposits are not sorted. The presence of marine fossiliferous lensoid beds, however, near the present summit of Lumaravi (Fouqué, 1879) indicates that sometime during its history the formation must have been covered by the sea.

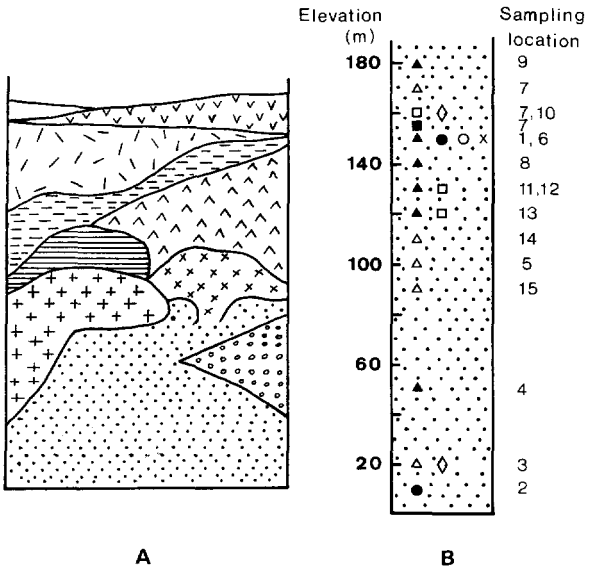

Figure 2. A. Generalized stratigraphic column of the Akrotiri area, after Pichler *et al.* (1980). (Symbols same as in Figure 1C). B. Columnar section of the Lumaravi-Archangelos pyroclastic rocks showing sampling locations and authigenic mineralogical compositions of the samples investigated at each location. Open triangle = (K,Ca)-rich clinoptilolite + mordenite + smectite + halite ± silica phase; solid triangle = (K,Ca)-rich clinoptilolite + mordenite + smectite ± silica phase; open square = K-rich clinoptilolite + smectite + silica phase ± mordenite ± halite; solid square = K-rich clinoptilolite + mordenite ± (silica phase or smectite); open circle = (K,Ca)-rich clinoptilolite + smectite + silica phase + kaolinite; solid circle = smectite; open diamond = halite ± kaolinite; X = (K,Ca)-rich clinoptilolite + mordenite + halite.

The original clasts were mainly ash and lapilli of vitric and crystal composition and of variable percentage of accidental angular blocks, as large as 15 cm in diameter, derived from the fragmentation of the pre-existing hornblende dacite. These unsorted volcaniclastic deposits were later consolidated to tuffs and lapilli tuffs or tuff breccia. The tuffs are white or shades of yellow, pink, and green and consist mainly of heulandite-group zeolites, mordenite, opal-CT, and smectite, along with rare pyrogenic quartz, plagioclase, and green-brown hornblende. The tuff breccia is composed mainly of gray to green dacitic lava blocks containing similar alteration products. Locally, however, they are only partly altered. The devitrification is less intense towards the core of the blocks, however, none of the samples analyzed contains fresh glassy groundmass. Unaltered plagioclase phenocrysts having oscillatory zoning (An_{40-53}) and microlitic plagioclase of similar composition are abundant; green-brown hornblende, clinopyroxene, and opaque minerals are more common in the dacitic blocks than in the tuffs.

←

Figure 1. A. Location of the Santorini group of islands, Aegean Sea, Greece. B. Caldera of Santorini group of islands. Framed area is depicted in C. C. Geological map of the Akrotiri area (after Pichler *et al.*, 1980). Numbered sample locations correspond to the following samples 1, S1-S5; 2, S13; 3, S16-S19; 4, S22; 5, S24; 6, S27; 7, S30-S34; 8, S35; 9, S36; 10, S40; 11, S43; 12, S45-S50; 13, S52, S53; 14, S62; 15, S66.

Table 1. Mineralogy of altered pyroclastic rocks from the Santorino volcano, Greece, determined by X-ray powder diffraction.

Sample	Elevation (m)	Mo	K-Cp	K-Ca-Cp	Smec	Crist	O-CT	Kaol	Hal	Qtz	Feld
S36	180	A	—	A	P	P	—	—	—	P	P
S34	170	P	—	A	T	T	—	—	P	—	P
S32	160	P	A	—	T	—	P	—	P	—	P
S40	160	—	—	—	—	—	—	A	P	—	—
S30	155	P	A	—	P	—	—	—	—	—	—
S30A	155	P	P	—	—	—	A	—	—	—	—
S1	150	—	—	—	A	—	—	—	—	—	P
S3	150	A	—	T	P	P	—	—	—	—	P
S4	150	P	—	A	P	T	—	—	—	—	P
S5	150	P	—	A	P	T	—	—	—	—	P
S6	150	—	—	T	P	—	A	P	—	—	—
S27	150	P	—	A	—	—	—	—	P	—	—
S35	140	P	—	A	P	—	—	—	—	—	T
S43	130	—	P	—	T	—	A	—	—	—	P
S46	130	P	—	A	P	P	—	—	—	—	P
S50	130	P	A	—	P	P	—	—	P	—	T
S45W	130	P	A	—	P	—	A	—	T	—	P
S45R	130	P	A	—	P	—	A	—	T	—	P
S48	130	P	A	—	P	—	P	—	P	—	P
S52	120	P	—	P	P	—	P	—	—	—	—
S53	120	P	A	—	P	P	—	—	—	—	P
S62	110	A	—	P	P	—	—	—	A	—	—
S24	100	P	—	A	T	—	—	—	P	—	—
S66	90	P	—	A	P	P	—	—	P	—	P
S22	50	P	—	A	P	—	—	—	—	—	—
S16	20	—	—	—	—	—	—	—	P	A	P
S17	20	P	—	A	T	P	—	—	T	—	P
S19	20	P	—	A	P	—	—	—	P	—	—
S13	10	—	—	—	P	—	—	—	—	A	P

Symbols: A = abundant; P = present; T = trace; — = not detected; Mo = mordenite; K-Cp = K-rich clinoptilolite; K-Ca-Cp = (K,Ca)-rich clinoptilolite; Smec = smectite; Crist = cristobalite; O-CT = opal-CT; Qtz = quartz; Feld = feldspar; Hal = halite; Kaol = kaolinite.

Table 2. Representative electron microprobe analyses of clinoptilolite and mordenite from altered pyroclastic rocks of the Lumaravi-Archangelos volcanics.

	K-rich clinoptilolite					(K,Ca)-rich clinoptilolite		Mordenite
	S32-2	S32-4	S32-6	S32-7	S43-2	S46-1	S46-3	S46-A
SiO_2	65.83	65.56	65.85	66.89	67.44	66.18	66.13	68.41
Al_2O_3	11.17	11.67	11.16	11.50	11.83	12.31	11.83	10.63
Fe_2O_3	0.04	0.00	0.01	0.00	0.00	0.00	0.01	0.35
MnO	0.00	0.02	0.00	0.00	0.01	0.00	0.00	0.00
MgO	0.32	0.52	0.20	0.30	0.33	0.37	0.15	0.00
CaO	1.44	1.49	1.42	1.34	1.60	2.29	2.08	1.61
Na_2O	0.41	0.62	0.69	0.33	1.02	0.74	0.79	3.52
K_2O	6.44	5.67	7.15	6.79	5.04	5.47	5.60	1.66
Total	85.65	85.55	86.48	87.15	87.27	87.36	86.59	86.18
	Unit-cell content based on 72 oxygen atoms							96 oxygens
Si	30.01	29.78	29.91	29.98	29.94	29.53	29.69	40.42
Al	6.00	6.25	5.98	6.07	6.19	6.47	6.28	7.40
Fe^{3+}	0.01	0.00	0.00	0.00	0.00	0.00	0.00	0.16
Mg	0.22	0.35	0.14	0.20	0.22	0.25	0.10	0.00
Ca	0.70	0.73	0.69	0.64	0.76	1.09	1.00	1.01
Na	0.36	0.54	0.61	0.28	0.88	0.64	0.68	4.02
K	3.74	3.29	4.15	3.88	2.85	3.11	3.22	1.24
Si:Al	5.00	4.76	5.00	4.94	4.84	4.56	4.72	5.46
(Ca + Mg):(Na + K)	0.22	0.28	0.17	0.20	0.26	0.36	0.28	0.19
E (%)	+1.2	+0.6	−6.7	+3.8	+8.9	+0.6	+2.8	+3.8

https://doi.org/10.1346/CCMN.1989.0370601 Published online by Cambridge University Press

The entire pyroclastic sequence is cut by an irregular, dense network of opal-CT-rich veins, which represent former flow paths of circulating fluids. It is important to note that some dacite and rhyodacite of the younger northern series has also been altered. Nicholls (1971) and Mann (1983) reported replacement of interstitial glass by fibrous aggregates of secondary minerals and zeolites as vesicle fillings. Hoefs (1980) also noted that the $\delta^{18}O$ values of some lavas from Santorini exceed +10‰ (vs. SMOW) and attributed this enrichment to secondary low-temperature alteration processes.

METHODS OF STUDY

About 60 samples of pyroclastic rocks were studied. Representative sampling locations are shown in Figure 1C, and a generalized stratigraphic column of the Akrotiri area is given in Figure 2A. At selected localities, short stratigraphic sections and more systematic sampling were made. Powder-pack mounts were used to produce random orientation for bulk X-ray diffraction (XRD) mineral analyses. For each sample, three mounts were prepared and investigated after heating at 260°, 400°, and 550°C to determine whether intensity reduction of the 020 and other XRD reflections of the heulandite-group zeolites occurred. The mounts were run at 1°2θ/min from 3° to 50°2θ using a Philips diffractometer and Ni-filtered CuKα radiation. For clay mineral identification, oriented mounts were prepared by sedimentation on a glass slide. Glycolation and heating at 490°C for 2 hr aided their identification. Relative abundances of authigenic minerals were estimated from the XRD patterns by using peak intensities. For samples of known chemical composition, the abundances were also calculated from the chemical analyses in terms of the chemistry of the minerals known to be present. Cristobalite was differentiated from opal-CT on the basis of their XRD patterns; opal-CT and cristobalite show characteristic peaks at 4.3 and 2.85 Å, respectively, along with their common peaks near 4.05–4.11 and 2.5 Å. Selected samples were examined in thin section and by scanning electron microscopy (SEM), using a JEOL JSM 820 instrument. Chemical analyses of the bulk samples were made using the Li tetraborate fusion method for Si and Ti and ICP on $HF/HClO_4$ solutions for the other elements. Elemental compositions were determined with a Link system energy-dispersive X-ray analyzer attached to a Cambridge Geoscan microprobe. Live time counts of 100 s and an acceleration voltage of 20 kV were the general analytical conditions. The quality of the zeolite analyses was calculated by spot checking the charge balance error

$$E = \frac{(Al + Fe) - (Na + K) - 2(Mg + Ca)}{(Na + K) + 2(Mg + Ca)} \times 100.$$

RESULTS

Authigenic mineralogy

Microscopic observations show that mainly the volcanic glass has undergone extensive alteration. The vitric matrix of the pyroclastic rocks has been generally replaced by one or more of the authigenic minerals, such as heulandite-group zeolites, mordenite, opal-CT, cristobalite, and clay minerals. Halite is also present in about half of the samples. No analcime was recognized, although Kanaris (1981) reported traces of this mineral in the Lumaravi-Archangelos volcanics.

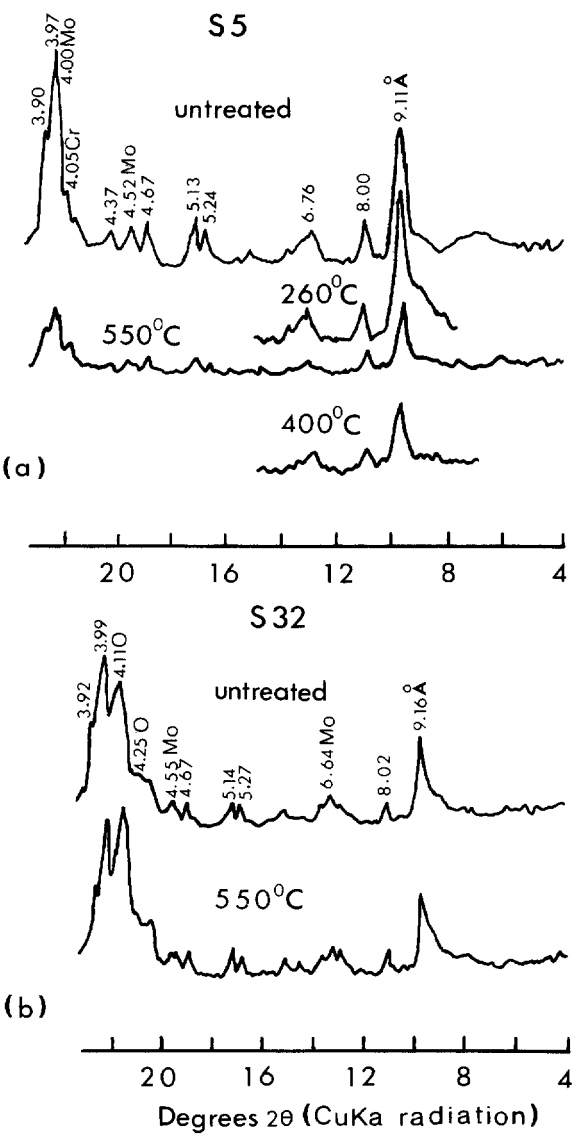

Figure 3. X-ray powder diffractograms of untreated and heated samples. (a) (K,Ca)-rich clinoptilolite-bearing sample S5; (b) K-rich clinoptilolite-bearing sample S32. All unlabeled peaks belong to heulandite-group minerals. Mo = mordenite; Cr = cristobalite; O = opal-CT. (d-values are in Ångstroms).

The mineralogical composition of the altered pyroclastic rocks, as determined by XRD analysis, is given in Table 1. It is evident from this table and Figures 1C and 2B that the outcrop distribution of authigenic sil-

https://doi.org/10.1346/CCMN.1989.0370601 Published online by Cambridge University Press

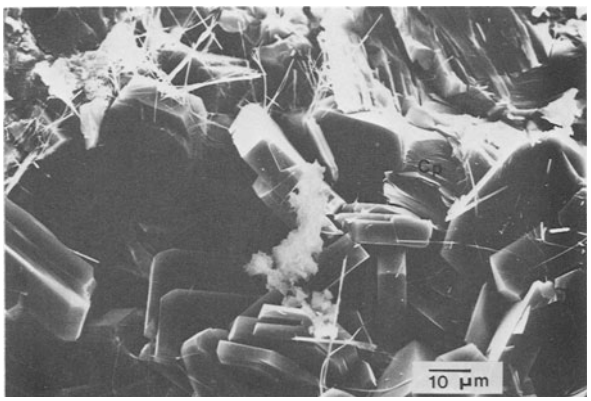

Figure 4. Scanning electron micrograph of sample S48, showing clinoptilolite. Note ragged morphology of some clinoptilolite crystals (Cp) and the presence of mordenite fibers over clinoptilolite crystals.

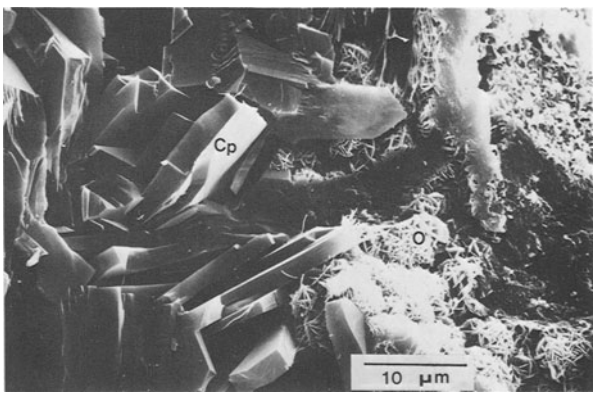

Figure 5. Scanning electron micrograph of sample S32, showing clusters of cross-radiating bladed opal-CT (O) developed over clinoptilolite crystals (Cp) showing ragged morphology.

icate minerals is random, inasmuch as no systematic vertical or lateral zonation was detected. The apparent decrease in silica minerals (opal-CT, cristobalite) towards the lower stratigraphic horizons probably is due to the selective collection of zeolite-rich samples.

Heulandite-group zeolites. Heulandite-group zeolites are the predominant zeolites in the Lumaravi-Archangelos pyroclastic rocks and are present from trace amounts to 60%. They commonly occur as microcrystalline aggregates making up most of the matrix in the altered tuffs and lapilli tuffs and as precipitates in cavities and veinlets. Glass shard pseudomorphs, partly or entirely filled by heulandite-group zeolites and other authigenic minerals, are more common in the altered dacitic blocks than in the tuffs and lapilli tuffs. The arrangement of the minerals in most of the glass shard pseudomorphs has the following form: a thin film of crystalline clay lines the outer walls, a layer of finely crystalline zeolites surrounds one or more layers of coarser tabular grains, which locally merge to close the cavities completely. Coprecipitated opal may be present in all zeolitic layers, however, globular opal is more common in the innermost parts of partly filled pseudomorphs. Heulandite-group zeolite crystals filling cavities of dissolved glass shards are commonly coarser (~30 μm) than those in the matrix and grow with their long axis perpendicular to the shard margin. SEM reveals that individual crystals have the characteristic tabular or platy monoclinic morphology and that some coexist with crystals showing ragged morphology (Figures 4, 5, and 11). Representative electron microprobe analyses of single crystals of heulandite-group zeolites, recalculated on the basis of 72 oxygen atoms, are given in Table 2. The sum of the exchangeable cationic charges in the unit cell of the analyses is only slightly less (generally by less than 0.5 units) than the number of R^3 cations in the tetrahedral sites, probably the result of volatization of light elements under the electron beam. In addition, the error (E) for the analyses is less than the commonly acceptable 10%; therefore, the analyses may be considered satisfactory.

The Si/Al ratios are 4.56–5.00, and using the classification scheme of Boles (1972), all the samples can be classified as clinoptilolite. The analyses reveal small but noticeable differences not only between clinoptilolite crystals encountered in different samples but between clinoptilolite crystals in the same sample (e.g., sample S32). The relative compositions of the exchangeable cations are shown in Figure 6. Note that the alkalis exceed Ca and that 60–80% of the exchangeable cations are potassium. The clinoptilolite in sample S46 is richer in Ca and poorer in alkalis than the clinoptilolite in samples S32 and S43 (Figure 6). Clinoptilolite from the latter sample plots in a marginal point between the field of clinoptilolite from sample S32 and that of the more (K,Ca)-rich clinoptilolite (sample S46). The Si/Al ratios are 4.56–4.72 for the (K,Ca)-rich clinoptilolite and 4.76–5.0 for the clinoptilolite in the other samples. These differences in their chemistry are consistent with their thermal behavior.

Heat treatments proposed by Mumpton (1960), Alietti (1972), and Boles (1972) were used to study their thermal properties. In most of the altered dacitic blocks (e.g., sample S32), the heulandite-group phase after overnight heating at 550°C retained 70–90% of its 020 peak intensity and is therefore clinoptilolite (heulandite of group 3) (Figure 3b). In most of the zeolitic tuffs and lapilli tuffs, however, after overnight heating at 550°C, the heulandite-group phase retained only 20–50% of its 020 intensity, even though according to its Si/Al ratio and low (0.26–0.36) divalent/monovalent cation ratio the zeolite can be classified as heulandite of group 3 (cf. Alietti *et al.,* 1977). The persistence of a portion of the 020 reflection at such temperatures characterizes heulandites of group 2 (Boles, 1972).

https://doi.org/10.1346/CCMN.1989.0370601 Published online by Cambridge University Press

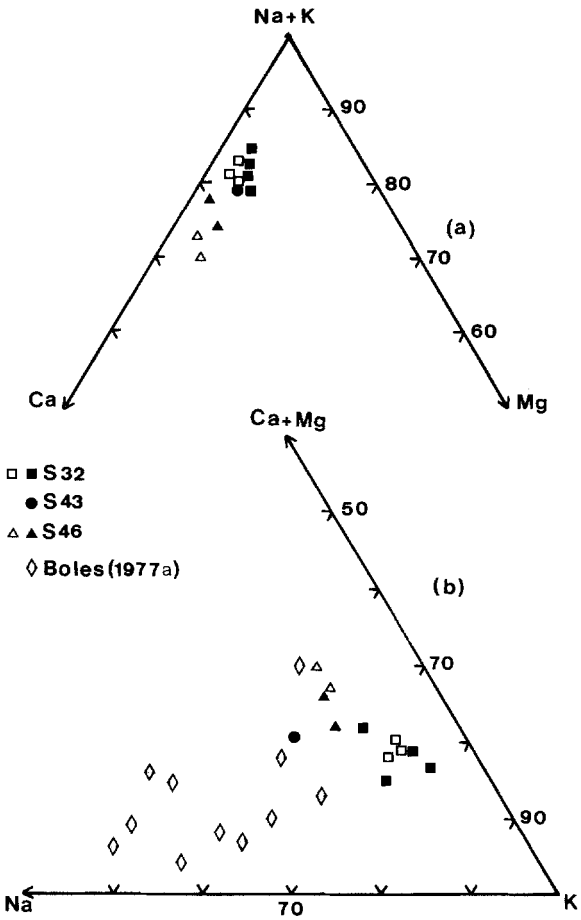

Figure 6. (a) (Na + K) : Ca : Mg plot and (b) (Ca + Mg) : Na : K plot for heulandite-group zeolites from pyroclastic rocks of Lumaravi-Archangelos volcanics. Samples S32 and S43 = K-rich clinoptilolite; sample S46 = (K,Ca)-rich clinoptilolite. Plots include analyses in addition to those given in Table 2. (Open symbols). Open diamonds in (b) represent compositions of K-rich clinoptilolite from deep-sea sediments given by Boles (1977a).

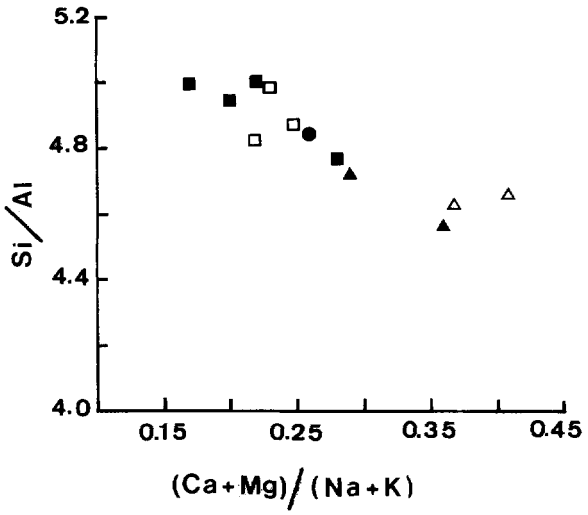

Figure 7. Si/Al vs. (Ca + Mg)/(Na + K) ratios of the heulandite-group zeolites from the pyroclastic rocks of the Lumaravi-Archangelos volcanics (symbols same as in Figure 6).

Nevertheless, the heat treatment of the present samples at 260°C for 2 hr and at 400°C overnight did not result in the appearance of a polymorphic phase (Figure 3a) (cf. Alietti, 1972; Boles, 1972). The behavior of these zeolites is similar to that of a Si-poor Na-clinoptilolite and of the intermediate heulandite-clinoptilolite described by Boles (1972, sample 9, Table 4) and Ratterman and Surdam (1981), respectively. Such intermediate thermal properties have been attributed by various workers (e.g., Shepard, 1961; Boles, 1972; Ratterman and Surdam, 1981) to the presence of clinoptilolite-heulandite mixtures, zoned crystals, or a chemically homogeneous alkali-rich heulandite. Where grain size permitted, many single crystals or crystal aggregates were analyzed in the (K,Ca)-rich clinoptilolite-bearing samples (S43 and S46), but no significant compositional variation or discernible zoning was found. The partial breakdown of the present (K,Ca)-rich clinoptilolite at 550°C and the absence of contracted phases at lower temperatures support the conclusion reached by several workers that slight differences in the type of cation play an important role in the thermal behavior of the heulandite-group zeolites.

Although the clinoptilolites examined here appear to have rather distinct Si/Al ratios and Ca and K contents, several analyses suggest a continuous variation in their composition and the (Ca + Mg)/(Na + K) ratio decreases with increasing Si/Al (Figure 7) (cf. Boles and Coombs, 1975). Ratterman and Surdam (1981) found no significant differences in the Si/(Al + Fe^{3+}) of the different heulandite-group zeolites, and from their data, this group of minerals appears to be best distinguished on the basis of their cation contents.

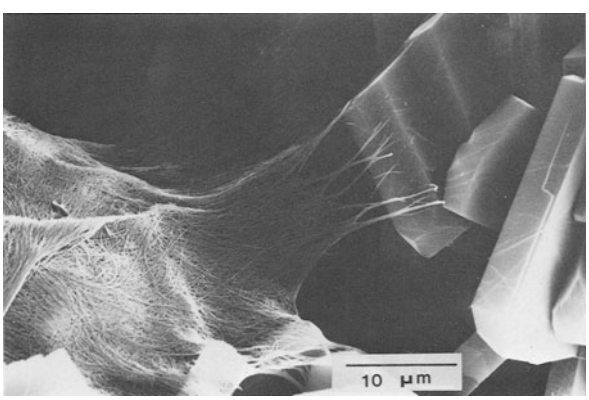

Figure 8. Scanning electron micrograph of sample S32 showing intertwined mordenite fibers and euhedral clinoptilolite crystals.

https://doi.org/10.1346/CCMN.1989.0370601 Published online by Cambridge University Press

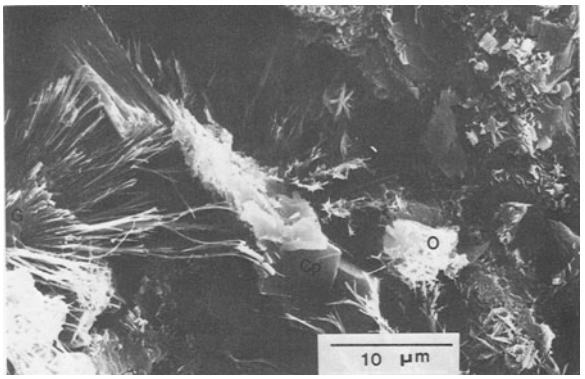

Figure 9. Scanning electron micrograph of sample S32, showing radiating mordenite fibers forming a 'whisk broom' texture. The mordenite fibers overlay a glass shard (G) (middle-left margin). Cp = clinoptilolite; O = opal-CT.

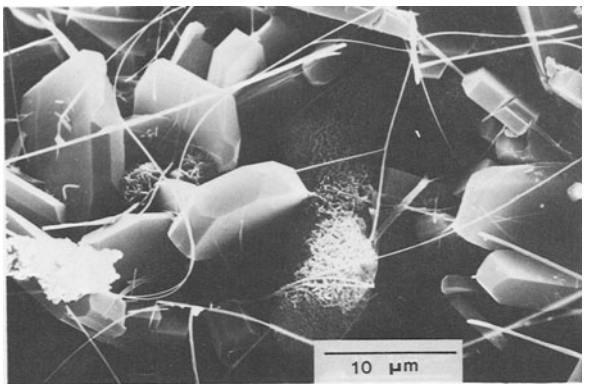

Figure 11. Scanning electron micrograph of sample S48, showing well-formed tabular clinoptilolite crystals and interstitial elongated blocks and clusters of cross-radiating opal-CT and thin fibers of mordenite draped over the clinoptilolite and opal-CT.

Compared with alkali-rich, heulandite-group zeolite compositions reported in the literature, the zeolites of the present study are similar only to some K-rich clinoptilolites from pelagic sediments, such as those described by Stonecipher (1978) and Boles (1977a) (Figure 6b).

Mordenite. Mordenite occurs in variable amounts in most of the samples examined and most commonly coexists with clinoptilolite, cristobalite, and smectite. Mordenite, due to its fine-grained nature, was identified by XRD and by crystal morphology using SEM. SEM shows that mordenite occurs as fibrous masses or as thin, scattered fibers. Individual fibers are less than 0.5 μm in diameter and about 20–80 μm long, curved, and commonly intertwine into mesh structures or "rats' nests" of the type described by Mumpton and Ormsby (1976) or occur in spider-web fashion coating or bridging the gaps between clinoptilolite crystals (Figure 8). Locally, coarser fibers radiate from a point forming a 'whisk broom' texture (Figure 9). Although mordenite was not generally observed as a direct alteration product of glass, SEM examination of sample S32 suggests that mordenite crystals formed from and around the relict glass (Figures 9 and 10). The mordenite crystals were too fine to be analyzed by the electron microprobe; however, analyses of a radial mineral aggregate in sample S46 yielded nearly identical results, close to mordenite. Optical observation was not conclusive in establishing the identity of this phase. The average composition of these spots is given in Table 2. The stoichiometric formula (on the basis of 96 oxygen atoms) is exceptional in that its 1.2 K- and 1 Ca-atoms per unit cell are outside the range (0.1–0.8 and 1.6–2.5, respectively) given by Gottardi and Galli (1985). The variation of the exchangeable cations in mordenite, however, must be larger as is evident from a triangular diagram given by Passaglia (1975, Figure 1) drawn from literature data.

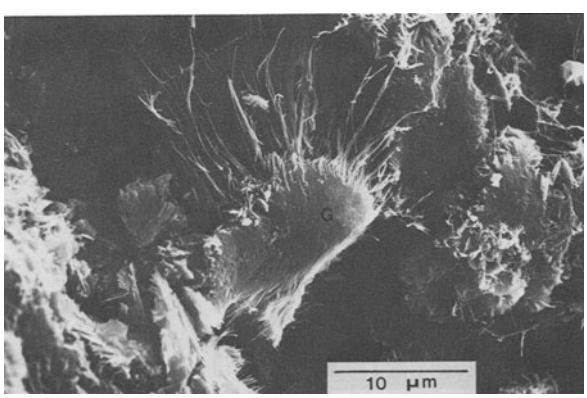

Figure 10. Scanning electron micrograph of sample S32, showing radiating mordenite fibers that apparently replaced the rim of a glass shard (G).

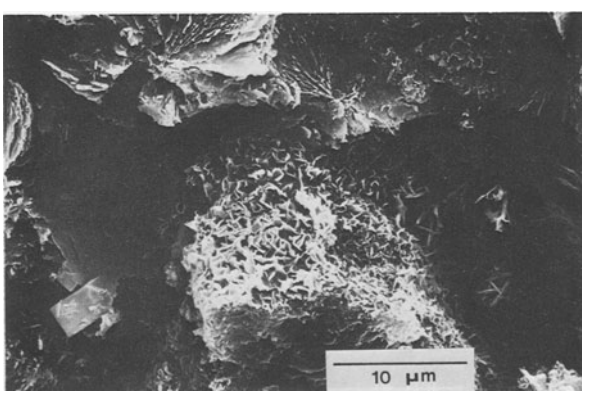

Figure 12. Scanning electron micrograph of sample S32. Smectite, showing characteristic flame-like structure, coexists with star-shaped clusters of opal-CT.

https://doi.org/10.1346/CCMN.1989.0370601 Published online by Cambridge University Press

Table 3. Representative bulk rock composition of altered dacitic blocks from the Lumaravi-Archangelos pyroclastic rocks.

	Unaltered dacite	Altered dacitic blocks			
	LA46[2]	S43	S30A	S50	S53
SiO_2	69.50	73.40	75.70	63.30	59.40
TiO_2	0.45	0.22	0.15	0.25	0.26
Al_2O_3	15.70	8.20	8.10	11.25	13.50
Fe_2O_3	1.30	1.80[1]	1.00[1]	1.86[1]	2.20[1]
FeO	1.56	—	—	—	—
MnO	0.08	0.17	0.01	0.04	0.05
MgO	1.20	0.90	0.60	1.20	1.60
CaO	2.90	1.30	1.90	2.30	2.30
Na_2O	4.59	2.20	2.40	4.16	3.40
K_2O	2.32	1.50	1.00	1.60	1.50
LOI	1.00	10.40	9.40	15.70	15.80
Total	100.57	100.09	100.26	101.66	100.01
Si/Al	3.91	7.90	8.26	4.97	3.89
Ca/(K + Na)	0.39	0.32	0.51	0.37	0.43
Zeolite[3]	—	K-Cp	K-Cp,Mo	K-Cp,Mo	K-Cp,Mo

[1] Total iron as Fe_2O_3.
[2] Nicholls (1971, Table 1).
[3] K-Cp = K-rich clinoptilolite; Mo = mordenite.

Silica minerals. Authigenic silica minerals range from trace amounts to about 75% of the sample and occur as secondary filling of fractures or voids or form crusts lining cavities and cementing the clasts of the pyroclastic rocks. SEM reveals that opal-CT commonly forms star-shaped clusters of cross-radiating bladed crystals (Figure 5), which locally form lepispheres or elongated blocks (Figure 11). On the basis of XRD data presented in Table 1, opal-CT more commonly coexists with smectite and K-rich clinoptilolite, especially in the opal-rich cross-cutting veins, whereas cristobalite more commonly coexists with (K,Ca)-rich clinoptilolite and mordenite in the tuffs. Quartz detected by XRD in three samples is considered to be pyrogenic.

Clay minerals. Smectite is present in most of the examined samples; it was identified from its 001 XRD reflection close to 14 Å which shifted to 17 Å on glycolation and collapsed on heating at 490°C for 2 hr. In a few samples, smectite is the main constituent; however, most tuffs contain no more than 15% smectite. SEM shows that smectite has typical flame-like structures with irregular outlines and commonly coexists with star-shaped clusters of opal-CT (Figure 12).

Kaolinite was identified as an accessory phase in one sample and as the main constituent in another. In both samples, the kaolinite is not very well crystallized. Not enough optical data were obtainable to give its paragenetic relationships with the authigenic minerals.

Halite. Halite is present in about half of the samples, and its abundance varies widely. It was identified from its XRD peaks at 2.82, 1.99, and 3.258 Å.

Host rock composition

Table 3 lists the chemical composition of unaltered and altered dacite samples along with the type of zeolite present in the latter. Table 4 lists the chemical composition of altered, opal-CT-rich samples and zeolitic tuffs along with the type of zeolite present in the latter materials. The most salient features of these tables are the extreme range of Si/Al ratios and the restriction of K-rich clinoptilolite to altered dacite samples and of (K,Ca)-rich clinoptilolite to altered tuffs and lapilli tuffs. The Si/Al ratios for the K-rich clinoptilolite-bearing rocks (Table 3) range from 3.89 to 8.26 (mean = 6.25) and for the (K,Ca)-rich clinoptilolite-bearing rocks (Table 4) from 3.63 to 4.78 (mean = 4.06).

The compositions of the altered dacitic blocks of the Lumaravi-Archangelos pyroclastic rocks and the unaltered dacitic flow (reported by Nicholls, 1971) (Table 3) are significantly different.

DISCUSSION

The alteration of the original dacite to the zeolite-rich (clinoptilolite, mordenite) rock (e.g., sample S53, Table 3) resulted in an increase in H_2O and MgO and a decrease in SiO_2, Na_2O, K_2O, Al_2O_3, and CaO. No data are available on the original bulk composition of the tuffs, the alteration of which led to the (K,Ca)-rich clinoptilolite-bearing rocks. A correlation of their present bulk composition with the textural relations of their authigenic minerals, however, suggests that zeolitization was accompanied by the same type of chemical modifications, with the exception of CaO, which increased with zeolitization. If the glass of the tuffs was initially similar in composition to the comparatively unaltered glass analyzed in the (K,Ca)-rich clinoptilolite-bearing sample S46 (Table 4), zeolitization apparently did not result in a significant change of the Si/Al ratio, inasmuch as this ratio is 4.29 and 4.06 in the glass and zeolitic tuff, respectively. The mean Ca/(K + Na) ratios of the halite-free, K-rich clinoptilolite-

https://doi.org/10.1346/CCMN.1989.0370601 Published online by Cambridge University Press

Table 4. Representative bulk rock compositions of altered opal-rich samples and zeolite-rich tuffs from the Lumaravi-Archangelos pyroclastic rocks.

	Altered, opal-rich samples					Zeolite-rich tuffs		
	Glass (S46)	S6	S16	S13	S1	S4	S5	S34
SiO_2	72.28	85.30	61.40	70.10	62.20	60.90	59.60	58.50
TiO_2	0.09	0.25	0.15	0.13	0.27	0.30	0.35	0.29
Al_2O_3	14.99	4.00	11.00	11.60	13.80	12.40	12.70	13.00
Fe_2O_3[1]	0.23	0.30	1.20	1.10	1.70	2.50	2.90	2.90
MnO	0.01	0.01	0.13	0.14	0.04	0.03	0.10	0.03
MgO	0.00	0.30	1.55	1.30	1.80	1.40	1.60	2.10
CaO	0.56	0.70	2.40	2.30	1.90	2.90	2.90	3.50
Na_2O	4.26	3.00	5.20	2.90	2.60	2.70	2.90	2.70
K_2O	6.27	1.80	5.60	2.80	1.70	1.80	1.90	2.00
LOI	—	5.10	10.20	6.50	13.00	13.90	13.60	15.50
Total	98.69	100.76	98.83	98.87	99.01	98.83	98.55	100.52
Si/Al	4.29	18.82	4.92	5.33	3.98	4.33	4.14	3.97
Ca/(K + Na)	0.04	0.13	0.20	0.36	0.40	0.59	0.55	0.68
Zeolite[2]	—	—	—	—	—	K-Ca-Cp Mo	K-Ca-Cp Mo	K-Ca-Cp Mo

[1] Total iron as Fe_2O_3.
[2] K-Ca-Cp = (K,Ca)-rich clinoptilolite; Mo = mordenite.

and (K,Ca)-rich clinoptilolite-bearing samples are 0.42 and 0.60, respectively. Thus, the initial compositional inhomogeneites apparently controlled the type of the heulandite-group zeolite that formed (cf. Boles and Coombs, 1975; Stonecipher, 1978).

The stages of alteration leading to the formation of zeolite-rich rocks are shown by comparing samples altered to different degrees. Samples S6, S16, S13, and S1 cannot be easily attributed to one of the original lithologies; however, the lack of zeolites and the presence of smectite and opal-CT in some of these samples suggest that they may represent initial alteration stages (Hay, 1963; Reynolds and Anderson, 1967; Henderson *et al.*, 1971; Reynolds, 1970). Inasmuch as no diagnostic XRD peaks for an authigenic phase were recognized in sample S16, its bulk chemistry probably reflects the composition of the dominant altered glass or noncrystalline silica deposited from the circulating fluids and pyrogenic feldspar and quartz. Textural evidence suggests that in a later stage, glass dissolved, and smectite and opal-CT formed to fill much of the pore space. Smectite was apparently the first mineral to crystallize, because the outer walls of most of the glass-shard pseudomorphs are lined with a thin layer of clay. The early formation of smectite was probably favored by a relatively low $(Na^+ + K^+)/H^+$ activity ratio in the pore fluid (Hemley, 1962). Subsequent alteration of glass to smectite would have raised the pH, a_{SiO_2}, and $(Na^+ + K^+)/H^+$ activity ratio, providing a chemical environment favorable for the formation of clinoptilolite (Hay, 1966; Hay and Sheppard, 1977; Hay and Guldman, 1987), depending on the initial composition. Inasmuch as SEM examination of some clinoptilolite-bearing samples shows that opal-CT coexists with early-formed smectite (Figure 12) and as spherules on top of clinoptilolite crystals (Figure 5), opal-CT probably continued to form at this stage and excess silica was probably present in the solution (Walton, 1975). The formation of K- and (K,Ca)-rich clinoptilolites may have caused an increase in the Na/K ratio in the remaining liquids. Solutions greatly enriched in Na relative to K apparently were unfavorable for clinoptilolite formation, and these zeolites were unstable with respect to the more Na-rich mordenite (see Hay, 1966; Hawkins *et al.*, 1978). At this stage, K-rich and (K,Ca)-rich clinoptilolites and opal-CT ceased to form, as indicated by the ragged morphology of some clinoptilolite crystals (Figures 4 and 5) and by the late precipitation of mordenite fibers over clinoptilolite crystals or globular bodies of opal-CT (Figures 4, 8, and 11). SEMs of sample S32 show that some of the mordenite fibers apparently grew by replacing the rims of glass shards (Figures 9 and 10), which could have been hydrated and leached of Al, as suggested by Gogishvili *et al.* (1973) and Hawkins *et al.* (1978).

The present study did not confirm the occurrence of analcime, traces of which in the Lumaravi-Archangelos pyroclastic rocks were reported by Kanaris (1981). According to Hay (1966) and the experimental work of Barrer and White (1952) and Coombs *et al.* (1959), mordenite and analcime may crystallize at the same temperature from solutions of similar composition, but at lower and higher pH, respectively. The formation of analcime from pre-existing alkalic, silicic zeolites has been correlated with a saline and alkaline environment (e.g., Sheppard and Gude, 1973) and also with a burial diagenetic setting (cf. Iijima and Utada, 1971). Inasmuch as hydration reactions led to the formation of the clay minerals and the zeolites must have consumed large quantities of water trapped in the Lu-

Table 4. Extended.

Zeolite-rich tuffs							
S46	S36	S17	S35	S19	S22	S24	S27
62.20	62.30	59.70	59.30	58.80	58.50	57.40	58.50
0.30	0.29	0.43	0.29	0.37	0.37	0.34	0.31
13.80	12.10	14.40	13.80	13.40	14.20	12.60	10.80
2.60	3.00	3.30	2.90	2.70	2.90	2.50	2.53
0.06	0.06	0.07	0.03	0.09	0.02	0.11	0.08
1.30	1.44	1.50	1.70	1.30	1.30	1.60	1.14
2.90	3.34	3.30	3.30	3.00	3.50	3.10	2.63
2.80	3.24	3.70	2.60	5.20	2.70	3.30	5.10
2.10	1.93	1.60	1.80	0.70	1.70	2.60	3.18
12.70	12.00	11.30	14.40	14.70	15.30	16.40	15.80
100.76	99.70	99.30	100.12	100.26	100.49	99.95	100.07
3.98	4.54	3.66	3.79	3.87	3.63	4.02	4.78
0.54	0.59	0.57	0.68	0.48	0.73	0.48	0.29
K-Ca-Cp Mo	Mo, K-Ca-Cp	K-Ca-Cp Mo	K-Ca-Cp Mo	K-Ca-Cp Mo	K-Ca-Cp Mo	K-Ca-Cp Mo	K-Ca-Cp Mo

maravi-Archangelos pyroclastic rocks, the remaining solutions probably became increasingly saline. The occurrence of halite in some of the examined samples indicates that salts might have been highly concentrated in such domains. The scarcity of analcime in the Lumaravi-Archangelos pyroclastic rocks suggests that the increased salinity of the fluids was rarely coupled with an increase in pH of the pore water, which would increase the Na^+/H^+ ratio and the solubility of SiO_2, favoring the crystallization of this zeolite.

The original pyroclastic material was possibly air laid onto the land surface, perhaps fairly close to the sea which subsequently covered the deposit. The authigenic silicate mineral assemblages probably resulted from a diagenetic alteration in a marine environment or in an open hydrologic system. Zeolites, however, such as clinoptilolite and mordenite, occur in both fresh and saline water environments. Their coexistence, coupled with the absence of phillipsite, also characterizes low-temperature hydrothermal alterations (Honda and Muffler, 1970; Iijima, 1974). The obvious evidence for a saline, alkaline environment, i.e., bedded saline minerals, has not been found in the Lumaravi-Archangelos pyroclastic rocks. Erionite, chabazite, and phillipsite which seem to be important indicators of depositional environments and which are common in saline, alkaline-lake deposits (Mumpton, 1978) were not found in the pyroclastic rocks studied. On the other hand, the presence of halite in the Lumaravi-Archangelos pyroclastic rocks imposes some problems, because to our knowledge, its occurrence is especially common in saline lakes (closed environments). Zeolite alteration zones in open-system deposits show more or less vertical sequences of authigenic silicate minerals, and zeolites produced in saline, alkaline lakes have relatively sharp or gradational lateral zones with rocks containing fresh glass, depending on the pH (Hay and Sheppard, 1977). As stated above, the alteration minerals in the Lumaravi-Archangelos deposit do not seem to be vertically zoned, the outcrop distribution of secondary mineral assemblages seems to be random, because adjacent samples at essentially the same stratigraphic horizon and derived from the same original lithology commonly contain contrasting mineral assemblages. This irregular distribution of zeolites and related minerals may be attributed to differences in factors controlling the alteration, such as localized heat flow, ionic activities in the stratal waters, and permeability of the pyroclastics in the circulation of fluids.

Inasmuch as the Lumaravi-Archangelos pyroclastic rocks were in a region of active heat production during and after their emplacement (cf. Nicholls, 1971; Ferrara *et al.*, 1980), their alteration features were probably not produced by cold water. Recent studies have shown that the geothermal gradient in the Akrotiri area (borehole 11, Figure 1C) is 4.7°C/100 m, but an even higher geothermal gradient (15.7°C/100 m) exists in the Thermia area between the surface and about 180 m (Kavourides *et al.*, 1982). Thermal springs of the sodium chloride type are known in the Thermia and Vlychadha areas, 3.5 km NE and SE of the Akrotiri village, respectively (Figure 1B). Kavourides *et al.* (1982), based on the chemistry at the thermal spring, drill hole, and well waters (Table 5) and the SiO_2 concentration and Na-K and Na-K-Ca geothermometers, suggested that the source aquifers may have had a temperature of 130°–140°C, but even higher temperatures (180°C) cannot be precluded. The hottest of the springs (Thermia) yields water at 52°C and contains 5.42% dissolved solids, an amount considerably higher than

Table 5. Chemical composition of selected hot spring, well, and borehole waters (ppm) from the Southern Santorini Island (Kavourides *et al.*, 1982).

	Thermia[1]	Vlychadha[1]	Akrotiri[2]	Akrotiri[3]
T (°C)	52	31.5	21	25
pH	6.65	7.70	7.50	6.10
Ca^{2+}	1,198.39	115.43	232.46	97.79
Mg^{2+}	1,685.38	92.42	158.08	30.64
Na^{+}	16,376.00	864.80	1,437.50	211.60
K^{+}	719.44	46.92	58.65	11.34
HCO_3^{-}	326.96	136.64	74.42	76.86
Cl^{-}	30,211.92	1,546.06	2,801.34	485.80
SO_4^{2-}	3,616.18	292.02	368.64	97.54
SiO_2	80.00	40.00	78.00	2.50
NH_4^{+}	0.20	0.30	1.54	0.75
B^{3+}	6.95	0.30	0.10	0.10
Fe^{2+}	n.d.	n.d.	0.20	0.08
Total salts	54,224.00	3,120.00	5,161.78	1,015.53

[1] Hot spring.
[2] Well.
[3] Borehole 11.

that of sea water. It also shows considerable differences in temperature and composition compared with the Vlychadha thermal spring, the borehole 11 water, and well waters of the Akrotiri area, which are of low salt content. Note that the geothermal fluid in Iceland is generally water of meteoric origin, and only in the extreme case of the Reykjanes high-temperature geothermal area, has the fluid the salinity of sea water (Kristmannsdóttir and Tómasson, 1978). Some oil field brines or thermal spring waters described by White (1957) have compositions similar in part to the Santorini thermal areas.

The differences in composition and temperature of the waters in the Akrotiri area suggest that the original hot, deep water was probably mixed with marine or ground water during its ascent through the various channels. Water that moved through short channels probably reached the surface at high temperature strongly enriched in salts, whereas water that followed longer paths reached the surface cooler and depleted in salts. This movement of hydrothermal waters of varying composition and temperature through the pyroclastic pile probably induced alteration in the mineral assemblages, the variation of which being governed by the relative distance of the sample to the circulation of the geothermal water.

Evidence for rapid flow, which created a uniform chemical environment, can be found in the widespread occurrence of cross-cutting opal-CT-rich veins and joints. Judging from the common occurrence of zeolites as a cement or cavity filling, however, and the variable degree of alteration over small areas in pyroclastic layers, the permeability did not favor rapid fluid movement throughout the formation. The importance of permeability in the alteration and the deposition of the different zeolite assemblages has been stressed by several authors (e.g., Boles, 1977b). The concept of high initial permeability, its subsequent decrease due to deposition of secondary minerals, and the formation of individual closed systems proposed by Keith and Staples (1985) seems to be compatible with the irregular distribution of zeolites and related minerals in the Lumaravi-Archangelos pyroclastic rocks. The alteration of the glassy tuffs to authigenic silicates by the geothermal water may have led gradually to the sealing of joints, fractures, and open spaces.

The permeability barriers imposed on the fluid flow may have subdivided the originally postulated open system into smaller closed systems. Then, as alteration progressed, some of the trapped water in each individual domain was consumed in hydration reactions, the water/rock ratio decreased, and the remaining fluid equilibrated at the new conditions (Michard, 1987). Each system further evolved by mainly solution-controlled reactions, and eventually adjacent samples developed different mineral assemblages. The irregular distribution of halite in the studied deposit indicates that the salinity of the fluids was different in the various sealed domains. Saturation in NaCl has been shown to be possible for systems undergoing hydration reactions (Trommsdorff and Skippen, 1987). Salts may have concentrated by such a process, and halite probably precipitated directly from solutions of appropriate composition in individual closed systems. The lack of zeolite species or other mineral species considered to be characteristic of a closed-system environment in the Lumaravi-Archangelos pyroclastic rocks may be explained by the low alkalinity of the trapped fluid. This suggestion is supported by the low pHs of the drill hole and well waters of the Akrotiri area, as well as by the pH of the hot spring waters of the Thermia and Vlychadha areas.

ACKNOWLEDGMENTS

We thank M. G. Audley-Charles for providing hospitality during our sabbatical at the Department of Geological Sciences, University College London, where much of the analytical work and the manuscript were completed, and D. Jachman, Geological Institut, University of Braunschweig, for providing the rock analyses. We are indebted to B. Roberts for allowing us to use the equipment at the Department of Geology, Birkbeck College, University of London, and to S. R. Hirons and A. D. Beard for technical assistance. Helpful discussions concerning this work with B. W. D. Yardley and G. D. Price are also greatly appreciated. The manuscript benefited greatly from reviews by R. A. Sheppard, B. Alexiev, E. Djourova, A. Iijima, and F. A. Mumpton.

REFERENCES

Alietti, A. (1972) Polymorphism and crystal-chemistry of heulandites and clinoptilolites: *Amer. Mineral.* **57**, 1448–1462.

Alietti, A., Brigatti, M. F., and Poppi, L. (1977) Natural Ca-rich clinoptilolites (heulandites of group 3): New data and review: *N. Jb. Miner. Mh.* **H. 11,** 493–501.

Barberi, F., Innocenti, F., Marinelli, C., and Mazzuoli, R. (1977) Vulcanismo e tettonica a placche: Esempi nell' area mediterranea: *Mem. Soc. Geol. It.* **13,** 327–358.

Barrer, R. M. and White, E. A. D. (1952) The hydrothermal chemistry of silicates. Part II. Synthetic crystalline sodium aluminosilicates: *J. Chem. Soc.* **286,** 1561–1571.

Boles, J. R. (1972) Composition, optical properties, cell dimensions, and thermal stability of some heulandite group zeolites: *Amer. Mineral.* **57,** 1463–1493.

Boles, J. R. (1977a) Zeolites in deep-sea sediments: in *Mineralogy and Geology of Natural Zeolites,* F. A. Mumpton, ed., Reviews in Mineralogy 4, Mineral. Soc. Amer., Washington, D.C., 137–163.

Boles, J. R. (1977b) Zeolites in low-grade metamorphic rocks: in *Mineralogy and Geology of Natural Geolites,* F. A. Mumpton, ed., Reviews in Mineralogy 4, Mineral. Soc. Amer., Washington, D.C., 103–136.

Boles, J. R. and Coombs, D. S. (1975) Mineral reactions in zeolitic Triassic tuff, Hokonui Hills, New Zealand: *Geol. Soc. Amer. Bull.* **86,** 163–173.

Coombs, D. S., Ellis, A. J., Fyfe, W. S., and Taylor, A. M. (1959) The zeolite facies, with comments on the interpretation of hydrothermal syntheses: *Geochim. Cosmochim. Acta* **17,** 53–107.

Davis, E. N. and Bastas, C. (1980) Petrology and geochemistry of the metamorphic system of Santorini: in *Thera and the Aegean World, I,* C. Doumas, ed., Tsiveriotis, Athens, 61–79.

Ferrara, G., Fytikas, M., Giuliani, O., and Marinelli, G. (1980) Age of the formation of the Aegean active volcanic arc: in *Thera and the Aegean World, II,* C. Doumas, ed., Tsiveriotis, Athens, 37–41.

Fouqué, F. (1879) *Santorin et ses Éruptions:* G. Maçon, Paris, 440 pp.

Fyticas, M., Giuliani, O., Innocenti, F., Marinelli, G., and Mazzuoli, R. (1976) Geochronological data of recent magmatism of the Aegean Sea: *Tectonophysics* **31,** 29–34.

Gottardi, G. and Galli, E. (1985) *Natural Zeolites:* Springer-Verlag, Berlin, 409 pp.

Gottardi, G. and Obradović, J. (1978) Sedimentary zeolites in Europe: *Fortschr. Miner.* **56,** 316–366.

Gogishvili, V. G., Khundadze, A. G., Politova, Yu. V., and Urushadze, V. V. (1973) Significance of the boundary layer of solution in the mordenite-analcime relation: *Geochem. Int.,* 1136–1144.

Hawkins, D. B., Sheppard, R. A., and Gude, A. J., 3rd (1978) Hydrothermal synthesis of clinoptilolite and comments on the assemblage phillipsite-clinoptilolite-mordenite: in *Natural Zeolites: Occurrence, Properties, Use,* L. B. Sand and F. A. Mumpton, eds., Pergamon Press, Elmsford, New York, 337–343.

Hay, R. L. (1963) Stratigraphy and zeolitic diagenesis of the John Day Formation of Oregon: *Univ. Calif. Pub. in Geol. Sci.* **42,** 199–262.

Hay, R. L. (1966) Zeolites and zeolitic reactions in sedimentary rocks: *Geol. Soc. Amer. Spec. Pap.* **85,** 130 pp.

Hay, R. L. and Guldman, S. G. (1987) Diagenetic alteration of silicic ash in Searles Lake, California: *Clays & Clay Minerals* **35,** 449–457.

Hay, R. L. and Sheppard, R. A. (1977) Zeolites in open hydrologic systems: in *Mineralogy and Geology of Natural Zeolites,* F. A. Mumpton, ed., Reviews in Mineralogy 4, Mineral. Soc. Amer., Washington, D.C., 93–102.

Hemley, J. (1962) Alteration studies in the system Na_2O-Al_2O_3-SiO_2-H_2O and K_2O-Al_2O_3-SiO_2-H_20: Geol. Soc. Amer. Abstracts for 1961: *Geol. Soc. Amer. Spec. Pap.* **68,** 196.

Henderson, J. H., Jackson, M. L., Syers, J. K., Clayton, R. N., and Rex, R. W. (1971) Cristobalite authigenic origin in relation to montmorillonite and quartz origin in bentonites: *Clays & Clay Minerals* **19,** 229–238.

Hoefs, J. (1980) Oxygen isotope composition of volcanic rocks from Santorini and Christiani: in *Thera and the Aegean World, I,* C. Doumas, ed., Tsiveriotis, Athens, 163–170.

Honda, S. and Muffler, L. J. P. (1970) Hydrothermal alteration in core from research drill hole Y-1, Upper Geyser Basin, Yellowstone National Park, Wyoming: *Amer. Mineral.* **55,** 1714–1737.

Iijima, A. (1974) Clay and zeolitic alteration zones surrounding Kuroko deposits in the Hokuroku District, northern Akita, as submarine hydrothermal-diagenetic alteration products: *Mining Geol. Special Issue* **6,** 267–289.

Iijima, A. and Utada, M. (1971) Present-day zeolitic diagenesis of the Neogene geosynclinal deposits in the Niigata oil field, Japan: in *Molecular Sieve Zeolites I, Advances in Chemistry Series,* **101,** R. F. Gould, ed., Amer. Chem. Soc., Washington, D.C., 342–349.

Innocenti, F., Manetti, P., Peccerillo, A., and Poli, G. (1979) Inner arc volcanism in NW Aegean Arc: Geochemical and geochronological data: *N. Jb. Min. Jg.,* 145–158.

Kanaris, J. (1981) Discovery of a sedimentary zeolitic deposit in Thera Island. Unpublished report, Institute of Geology and Mineral Exploration, Athens, 16 pp. (in Greek).

Kavourides, Th., Karidakis, G., Kolios, N., Kouris, D., and Fytikas, M. (1982) Geothermal research in Santorini Island: Unpublished report, Institute of Geology and Mineral Exploration, Athens, 16 pp. (in Greek).

Keith, T. E. and Staples, L. W. (1985) Zeolites in Eocene basaltic pillow lavas of the Siletz River Volcanics, Central Coast Range, Oregon: *Clays & Clay Minerals* **33,** 135–144.

Kristmannsdóttir, H. and Tómasson, J. (1978) Zeolite zones in geothermal areas in Iceland: in *Natural Zeolites: Occurrence, Properties, Use,* L. B. Sand and F. A. Mumpton, eds., Pergamon Press, Elmsford, New York, 277–284.

Mann, A. C. (1983) Trace element geochemistry of high alumina basalt-andesite-dacite-rhyodacite lavas of the main volcanic series of Santorini volcano, Greece: *Contrib. Mineral. Petrol.* **84,** 43–57.

Michard, G. (1987) Controls of the chemical composition of geothermal waters: in *Chemical Transport in Metasomatic Processes,* H. C. Helgeson, ed., D. Reidel Publ., Dordrecht, The Netherlands, 323–353.

Mumpton, F. A. (1960) Clinoptilolite redefined: *Amer. Mineral.* **45,** 351–369.

Mumpton, F. A. (1978) Natural zeolites: A new industrial mineral commodity: in *Natural Zeolites: Occurrence, Properties, Use,* L. B. Sand and F. A. Mumpton, eds., Pergamon Press, Elmsford, New York, 3–27.

Mumpton, F. A. and Ormsby, W. C. (1976) Morphology of zeolites in sedimentary rocks by scanning electron microscopy: *Clays & Clay Minerals* **24,** 1–23.

Nicholls, I. A. (1971) Petrology of Santorini volcano, Cyclades, Greece: *J. Petrology* **12,** 67–119.

Papastamatiou, J. (1958) Sur l'âge des calcaires cristallins de l'île de Théra (Santorini): *Bull. Geol. Soc. Greece* **3,** 104–113.

Passaglia, E. (1975) The crystal chemistry of mordenite: *Contrib. Mineral. Petrol.* **50,** 65–77.

Pichler, H. and Kussmaul, S. (1972) The calc-alcaline volcanic rocks of the Santorini Group (Aegean Sea, Greece): *N. Jb. Miner. Abh.* **116,** 268–307.

Pichler, H., Günther, D., and Kussmaul, S. (1980) Geological map of Thera Island, scale 1:50.000, Institute of Geology and Mineral Exploration, Athens, Greece.

Ratterman, N. G. and Surdam, R. C. (1981) Zeolite mineral

reactions in a tuff in the Laney Member of the Green River Formation, Wyoming: *Clays & Clay Minerals* **29,** 365–377.

Reck, H. (1936) Santorin—Der Werdegang eines Inselvulkans und sein Ausbruch 1925–1928. 1, XXXVI. 187 pp.; 2, XV. 353 pp. Berlin.

Reynolds, W. R. (1970) Mineralogy and stratigraphy of Lower Tertiary clays and claystones of Alabama: *J. Sediment. Petrol.* **40,** 829–838.

Reynolds, R. C., Jr. and Anderson, D. M. (1967) Cristobalite and clinoptilolite in bentonite beds of the Colville Group, northern Alaska: *J. Sediment. Petrol.* **37,** 966–969.

Shepard, A. O. (1961) A heulandite-like mineral associated with clinoptilolite in tuffs of Oak Springs Formation, Nevada Test Site, Nye Co., Nevada: in Geological Survey Research, *U.S. Geol. Surv. Prof. Pap.* **424-C,** C320–C322.

Sheppard, R. A. (1971) Zeolites in sedimentary deposits of the United States—A review: in *Molecular Sieve Zeolites I, Advances in Chemistry Series,* **101,** R. F. Gould, ed., Amer. Chem. Soc., Washington, D.C., 279–310.

Sheppard, R. A. and Gude, A. J., 3rd (1973) Zeolites and associated authigenic silicate minerals in tuffaceous rocks of the Big Sandy Formation, Mohave County, Arizona: *U.S. Geol. Surv. Prof. Pap.* **830,** 36 pp.

Stonecipher, S. A. (1978) Chemistry and deep-sea phillipsite, clinoptilolite, and host sediments: in *Natural Zeolites: Occurrence, Properties, Use,* L. B. Sand and F. A. Mumpton, eds., Pergamon Press, Elmsford, New York, 221–234.

Tataris, A. A. (1964) The Eocene in the semi-metamorphosed basement of Thera Island: *Bull. Geol. Soc. Greece* **6,** 232–238, (in Greek).

Trommsdorff, V. and Skippen, G. (1987) Metasomatism involving fluids in CO_2-H_2O-NaCl: in *Chemical Transport in Metasomatic Processes,* H. C. Helgeson, ed., D. Reidel Publ., Dordrecht, The Netherlands, 133–152.

Walton, A. W. (1975) Zeolitic diagenesis in Oligocene volcanic sediments, Trans-Pecos Texas: *Geol. Soc. Amer. Bull.* **86,** 615–624.

White, D. E. (1957) Magmatic, connate, and metamorphic waters. *Geol. Soc. Amer. Bull.* **68,** 1659–1682.

(Received 15 November 1988; accepted 20 April 1989; Ms. 1850)